Received: 5 May 2022 | Revised: 6 July 2022 | Accepted: 14 July 2022

DOI: 10.1002/hon.3050

ORIGINAL ARTICLE

WILEY

NR1H3 (LXRα) is associated with pro-inflammatory macrophages, predicts survival and suggests potential therapeutic rationales in diffuse large b-cell lymphoma

Maria Carmela Vegliante[1] | Saveria Mazzara[2] | Gian Maria Zaccaria[1] | Simona De Summa[3] | Flavia Esposito[4,5] | Federica Melle[2] | Giovanna Motta[2] | Maria Rosaria Sapienza[2] | Giuseppina Opinto[1] | Giacomo Volpe[1] | Antonella Bucci[1] | Grazia Gargano[1,5] | Anna Enjuanes[6] | Valentina Tabanelli[2] | Stefano Fiori[2] | Carla Minoia[1] | Felice Clemente[1] | Antonio Negri[1] | Alessandro Gulino[7] | Gaia Morello[8] | Anna Scattone[9] | Alfredo F. Zito[9] | Stefania Tommasi[3] | Claudio Agostinelli[10,11] | Umberto Vitolo[12] | Annalisa Chiappella[13] | Anna Maria Barbui[14] | Enrico Derenzini[15,16] | Pier Luigi Zinzani[11,17] | Beatrice Casadei[11,17] | Alfredo Rivas-Delgado[18] | Armando López-Guillermo[18] | Elias Campo[19] | Antonio Moschetta[20] | Attilio Guarini[1] | Stefano A. Pileri[2] | Sabino Ciavarella[1]

[1]Hematology and Cell Therapy Unit, IRCCS-Istituto Tumori 'Giovanni Paolo II', Bari, Italy

[2]Division of Hematopathology, European Institute of Oncology, IRCCS, Milan, Italy

[3]Molecular Diagnostics and Pharmacogenetics Unit, IRCCS-Istituto Tumori 'Giovanni Paolo II', Bari, Italy

[4]Department of Mathematics, University of Bari Aldo Moro, Bari, Italy

[5]INDAM-GNCS Research Group, Rome, Italy

[6]Unitat de Genòmica, Institut d'Investigacions Biomèdiques August Pi i Sunyer (IDIBAPS), Barcelona; CIBERONC, Barcelona, Spain

[7]Cogentech srl Società Benefit, FIRC Institute of Molecular Oncology (IFOM), Milan, Italy

[8]Department of Health Sciences, Tumor Immunology Unit, University of Palermo School of Medicine, Palermo, Italy

[9]Pathology Department, IRCCS-Istituto Tumori 'Giovanni Paolo II', Bari, Italy

[10]Haematopathology Unit, IRCCS Azienda Ospedaliero-Universitaria di Bologna, Bologna, Italy

[11]Department of Experimental, Diagnostic and Specialty Medicine, University of Bologna, Bologna, Italy

[12]Candiolo Cancer Institute, FPO-IRCCS, Candiolo, Italy

[13]Division of Hematology and Stem Cell Transplantation, Fondazione IRCCS Istituto Nazionale dei Tumori, Milano, Italy

[14]Department of Oncology and Hematology, Azienda Socio-Sanitaria Territoriale Papa Giovanni XXIII, Bergamo, Italy

[15]Onco-Hematology Division, European Institute of Oncology IRCCS, Milan, Italy

[16]Department of Health Sciences, University of Milan, Milan, Italy

[17]Istituto di Ematologia "Seràgnoli", IRCCS Azienda Ospedaliero-Universitaria di Bologna, Bologna, Italy

[18]CIBERONC, Barcelona, Spain; Hematology Department, Hospital Clínic, Barcelona; IDIBAPS, Barcelona, Spain

Stefano A. Pileri and Sabino Ciavarella contributed equally as last authors.

[19]CIBERONC, Barcelona, Spain; Haematopathology Unit, Pathology Department, Hospital Clínic, Barcelona; University of Barcelona, Barcelona, Spain

[20]Department of Interdisciplinary Medicine, University of Bari Aldo Moro, Bari, Italy

Correspondence
Sabino Ciavarella, Hematology and Cell Therapy Unit, IRCCS-Istituto Tumori 'Giovanni Paolo II', Bari, 70124, Italy.
Email: s.ciavarella@oncologico.bari.it

Funding information
Italian Ministry of Health - "Ricerca Corrente"; Associazione Italiana per la Ricerca sul Cancro (AIRC)
Open access funding provided by BIBLIOSAN.

Abstract

The role of macrophages (Mo) and their prognostic impact in diffuse large B-cell lymphomas (DLBCL) remain controversial. By regulating the lipid metabolism, Liver-X-Receptors (LXRs) control Mo polarization/inflammatory response, and their pharmacological modulation is under clinical investigation to treat human cancers, including lymphomas. Herein, we surveyed the role of LXRs in DLBCL for prognostic purposes. Comparing bulk tumors with purified malignant and normal B-cells, we found an intriguing association of *NR1H3*, encoding for the LXR-α isoform, with the tumor microenvironment (TME). CIBERSORTx-based purification on large DLBCL datasets revealed a high expression of the receptor transcript in M1-like pro-inflammatory Mo. By determining an expression cut-off of *NR1H3*, we used digital measurement to validate its prognostic capacity on two large independent on-trial and real-world cohorts. Independently of classical prognosticators, *NR1H3*^{high} patients displayed longer survival compared with *NR1H3*^{low} cases and a high-resolution Mo GEP dissection suggested a remarkable transcriptional divergence between subgroups. Overall, our findings indicate *NR1H3* as a Mo-related biomarker identifying patients at higher risk and prompt future preclinical studies investigating its mouldability for therapeutic purposes.

KEYWORDS
deconvolution, diffuse large B-cell lymphoma, gene expression profiling, liver X receptors, microenvironment

1 | INTRODUCTION

Diffuse large B cell lymphoma (DLBCL) represents a highly heterogeneous disease calling for a more accurate risk stratification at diagnosis and improvement of first-line immunochemotherapy.[1–3] Sequencing studies refined the stratification of molecular subgroups of DLBCL characterized by druggable genetic aberrations[4–6] and prognostic components of tumor microenvironment (TME).[7,8] Among these, tumor-infiltrating macrophages (Mo) are regarded as a functionally heterogeneous immune population whose association with patient prognosis remains controversial due to the insufficient reproducibility of cell-specific, robust functional biomarkers.[9] Moreover, owing to the lack of unique druggable targets, no data are currently available that support rationales for Mo-directed strategies of immunomodulation in DLBCL.

Accumulating evidences indicate that critical events in TME are influenced by oxygen tensions, cytokine gradients, and nutrient alteration including lipid and cholesterol metabolism.[10] The latter is controlled by two isoforms of the Liver-X-Receptors (LXRs),[11,12] namely LXRα and LXRβ, that are mainly expressed in cells with high cholesterol turnover, such as Mo, in which they regulate viability, polarization and inflammatory response.[12,13] Moreover, anti-proliferative effects have been described in solid cancers as an effect of TME changes upon direct LXR pharmacological modulation.[14,15] Many LXR agonists have been pre-clinically tested with therapeutic purposes and provided controversial results due to different underlying biology in different cancers.[15,16] For instance, RGX-104, a first-in-class oral LXR agonist, is being tested in a phase 1b/2 trial including solid tumors and aggressive lymphomas.[17] The anti-tumor properties of RGX-104 correlate with critical changes in TME involving myeloid-derived suppressor cells and Mo.[18] However, no data are available on LXR biology in lymphoproliferative disorders and, particularly, in DLBCL.

Here, we explored potential association of LXRs with specialized subsets of tumor-infiltrating immune cells in DLBCL. By systematic deconvolution of gene expression profiling (GEP) data from large patient cohorts, we revealed a striking correlation of LXRα transcript (encoded by *NR1H3* gene) with a subset of pro-inflammatory Mo in patients displaying better clinical outcome. Conversely, patients with low levels of *NR1H3* expression showed inferior survival, independently of standard prognosticators. These observations were further validated by NanoString technology in two additional independent

DLBCL cohorts, supporting the idea of *NR1H3* as a potential biomarker of a transcriptionally-restricted Mo subsets that might be susceptible to pharmacological agonism, paving the way for new strategies of immunomodulation in DLBCL.

2 | MATERIAL AND METHODS

2.1 | Patients characteristics and cohorts

Deconvolution and survival analyses were performed on a discovery set obtained by pooling 314 DLBCL with comprehensive clinical and molecular information from three different GEP datasets (GSE10846, GSE34171 and GSE98588).[2,6,19] For prognostic validation, we used data from 175 patients with advanced-stage, nodal, de novo DLBCL, not otherwise specified, enrolled in two different clinical trials,[20,21] and an additional real-world (RW, n = 146) cohort collected from four Institutions (IRCCS - Istituto Tumori 'Giovanni Paolo II' of Bari, Italy; Istituto di Ematologia "Seràgnoli", IRCCS Azienda Ospedaliero-Universitaria di Bologna, Italy; IRCCS-European Institute of Oncology of Milan, Italy; Hospital Clinic, Barcelona, Spain). Diagnostic tumor samples were obtained before any treatment.

The study was conducted according to the Declaration of Helsinki and all patients signed a dedicated informed consent. All cases were reviewed by experienced hematopathologists (CA, SF, SAP, AS, EC, VT, AFZ). An additional public DLBCL series (GSE117556) using a different microarray platform (Illumina)[22] was used to validate the prognostic value of *NR1H3*. Clinical characteristics of patients from different cohorts are summarized in Table 1. The whole study workflow is schematized in Figure S1.

2.2 | *NR1H3* and *NR1H2* expression analysis

Raw data from different public datasets of DLBCL cases, cell line and normal B-cells[2,6,19,23–25] were used to generate expression profiles by RMAExpress v1.2.0 (Robust Multi-Array Average). Multiple probes were collapsed into unique genes by selecting those with the maximum value for each gene. Expression values were log2 transformed, and *NR1H3* and *NR1H2* transcripts abundance extracted for further analysis.

2.3 | CIBERSORTx

CIBERSORTx (http://cibersortx.stanford.edu) was run on publicly available datasets to calculate the proportions (at 1000 permutation per run) and to obtain GEPs (by Group-Mode imputation) of immune cytotypes in the LM22 signature. Gene expression profiling data (Affymetrix Microarray) from the discovery set were summarized and normalized using the Robust Multi-array Averaging method by means of *affy* (version 1.70.0) package in R (version

TABLE 1 Clinical and molecular features of diffuse large B-cell lymphomas (DLBCL) cohorts

	Discovery dataset (N = 314)	DLBCL validation set (on trial) (N = 175)	DLBCL validation set (real-world) (N = 146)	GSE117556 (N = 893)
IPI range				
High	49 (15.6%)	47 (26.9%)	16 (11.0%)	156 (17.5%)
High-Int	68 (21.7%)	128 (73.1%)	40 (27.4%)	268 (30.0%)
Low	121 (38.5%)	0 (0%)	51 (34.9%)	244 (27.3%)
Low-Int	76 (24.2%)	0 (0%)	39 (26.7%)	225 (25.2%)
COO				
ABC	142 (45.2%)	38 (21.7%)	57 (39.0%)	253 (28.3%)
GCB	125 (39.8%)	103 (58.9%)	63 (43.2%)	511 (57.2%)
UC	47 (15.0%)	34 (19.4%)	25 (17.1%)	129 (14.4%)
NR1H3				
High	266 (84.7%)	154 (88.0%)	122 (83.6%)	837 (93.7%)
Low	48 (15.3%)	21 (12.0%)	24 (16.4%)	56 (6.3%)
Gender				
Female	102 (32.5%)	83 (47.4%)	34 (23.3%)	396 (44.3%)
Male	149 (47.5%)	92 (52.6%)	40 (27.4%)	497 (55.7%)
Age				
Median [Min, Max]	62.0 [17.0, 92.0]	52.0 [18.0, 65.0]	64.2 [16.8, 87.7]	64.7 [20.8, 86.1]

Abbreviations: COO, cell of origin; IPI, international prognostic index.

4.1.0, R Core Team 2020, Vienna, Austria, https://www.R-project.org). The GSE117556 dataset (Illumina platform) was normalized by *limma* (version 3.48.0) package in R before deconvolution. Bulk-mode batch correction (B-mode) was applied to all the datasets. GSE125966, GSE145043[26] and Schmitz *et al*.[5] RNA-seq data were analyzed using the authors' normalization settings including counts per million, transcripts per million and fragments per kilobase of transcript per million (ragments per kilobase of transcript per million) space, respectively.

2.4 | RNA in situ hybridization and immunohistochemistry (IHC)

RNA in situ hybridization and IHC were performed using Human *NR1H3* transcript (Hs-NR1H3; Cod.440881) and CD68-antibody (clone PG-M1 DAKO) respectively (Supplementary Methods).

2.5 | NanoString-based gene expression quantification

Total RNA was extracted from formalin-fixed paraffin-embedded (FFPE) sections of DLBCL cases as previously reported.[27] The nCounter Digital Analyzer NanoString Technology was used for Cell-of-origin (COO) assignment (Lymph2Cx assay) and for digital measurement of *NR1H3* expression, according to manufacturer's instructions. A custom probe for *NR1H3* (5′-CCCATGGACAC CTACATGCGTCGCAAGTGCCAGGAGTGTCGGCTTCGCAAATGCC GTCAGGCTGGCATGCGGGAGGAGTGTGTCCTGTCAGAAGAACAG A-3′) and five housekeeping genes (UBXN4, TRIM56, WDR55, R3HDM1, ISY1) were used. All data were normalized using NanoStringNorm (version 1.2.1.1) package in R software, as previously described.[7]

2.6 | Tissue microarrays (TMA) and immunohistochemical evaluation of CD68

Tissue microarrayswere constructed by selecting three cores of 0.6-mm diameter from representative areas of FFPE blocks relative to 64 cases selected among the on-trial validation cohort and 2μm-section stained with CD68 (Clone PG-M1, dilution 1:8, courtesy of Prof. Brunangelo Falini). Further details are reported in Supplementary Methods.

2.7 | Normalization and DEG

The DLBCL discovery set was generated by pooling Affymetrix-HG133plus2 raw data from three different datasets (GSE10846, GSE34171 and GSE98588) processed as a unique expression matrix by R package *affy* (version 1.66) to reduce batch effect. All cases were collected in real world studies and homogeneously treated by standard immuno-chemotherapy.

The high-resolution mode of CIBERSORTx was applied to virtually purify macrophage GEP (M0, M1, M2 populations) and a list of differentially expressed genes (DEG) was obtained by comparing $NR1H3^{high}$ and $NR1H3^{low}$ cases separated using the prognostic cut-off (Supplementary Methods). *Limma* R package (version 3.48.0) was used to perform DEG analysis and *clusterProfiler* R package (version 4.0.2) to perform Gene Ontology (GO) over-representation tests.

2.8 | *In vitro* macrophage polarization and treatment

THP-1 cell line was obtained from American Type Culture Collection (Manassas, VA, USA) and grown in Roswell Park Memorial Institute 1640 (Gibco, Thermo Fisher Scientific) supplemented with 10% heat-inactivated fetal bovine serum, 1% Penicillin-Streptomycin (10,000 U/mL, 10mg respectively) (Sigma Aldrich), 2 mM glutamine (Gibco) and 0.05 mM of 2-mercaptoethanol (Sigma Aldrich). M1- and M2-polarized Mo were generated from THP-1 cells as previously described.[28] The complete protocol is detailed in Supplementary Materials.

2.9 | Statistical analysis

Dot plots for GO analysis representation, heatmaps, correlation matrix plots and survival analysis were produced using R statistical software. *p*-values among continuous variables were calculated by Mann–Whitney test or independent Student's *t*-test. Further details are provided in Supplementary Methods.

3 | RESULTS

3.1 | *NR1H3* (LXRα) is up-regulated in DLBCL TME and associated with M1-like Mo

To explore the role of LXRs in DLBCL, we first analyzed the transcriptional levels of the two LXR isoforms (LXRα and LXRβ), encoded by *NR1H3* and *NR1H2*, respectively, in different public GEP datasets of bulk DLBCL as well as in malignant cells purified from lymph node, DLBCL cell lines and normal B-cells. We observed that *NR1H3* expression was significantly higher in samples derived from whole biopsies as compared with purified tumor cells, malignant cell lines and normal B cells ($p<10^{-3}$). This finding suggested that major contribution to *NR1H3* expression is attributable to TME rather than tumor component. Conversely, no significant differences were observed in *NR1H2* across datasets (Figure 1A).

To inspect which cytotype displays the highest *NR1H3* expression within TME, we retrieved publicly GEP arrays from a discovery

set of 314 cases and four additional independent datasets, and applied CIBERSORTx to study the gene expression patterns. Among 22 tumor-infiltrating immune cell types resolved, Mo - especially the M0/M1 fraction - appeared to reproducibly express the highest levels of *NR1H3*. γ/δ T cells and neutrophils showed considerable *NR1H3* abundance, but with no reproducibility across different cohorts. Conversely, M2 Mo, B- and T-cell subsets as well as other components of innate immunity, such as natural killer, dendritic and mast cells, displayed negligible transcript levels (Figure 1B). This observation was also confirmed by a correlation analysis between *NR1H3* levels and cell fractions, with the M0/M1 Mo subset displaying the highest correlation in all datasets (Supplementary Figure 2A–B). To corroborate these findings, we performed a simultaneous *in situ* detection of CD68 and *NR1H3* in prototypical DLBCL biopsies. While no *NR1H3* signal was detected in malignant B cells, we observed a variable co-localization with CD68, as a selective histiocyte marker (Figure 1C). The amount of $CD68^{+}/NR1H3^{+}$ cells largely varied among cases, suggesting that, despite showing a similar phenotype, Mo sub-populations with different transcriptional programs might coexist within the TME.

We proceeded to validate the observation of *NR1H3* expression being restricted to M0/M1 Mo levels in different populations of *in vitro* polarized Mo. Consistently, THP-1 cells, polarized toward a M1-like state and featuring a typical over-expression of *CXCL10* and *IL-1β*, displayed significantly higher *NR1H3* expression (p-value = 0.001) as compared with the classical $CD206^{+}/CD163^{+}$ M2 phenotype (Figure 1D, Supplementary Figure S3). This was also reflected by substantial upregulation of *ABCA1*, the main *NR1H3* target, in M1 Mo only, thus confirming our observation of LXRα restriction to M1 Mo.

3.2 | Patients expressing low *NR1H3* levels display unfavorable survival

Given the potential albeit controversial prognostic impact of Mo and the TME in DLBCL, we assessed the prognostic value of *NR1H3* in the discovery cohort. To do so, we applied maximally selected rank statistics to dichotomize patients on the basis of LXRα expression into $NR1H3^{high}$ (n = 266) and $NR1H3^{low}$ (n = 48) subgroups. Survival analysis demonstrated $NR1H3^{low}$ patients associated with a significantly shorter overall survival (OS; p-value<0.0001, median 5-year OS, $NR1H3^{high}$ 75% vs. $NR1H3^{low}$ 25%) (Figure 2A). Also, a multivariate analysis indicated that the prognostic power of LXRα was independent of international prognostic index (IPI) and COO (Figure 2A). Notably, $NR1H3^{high}$ and $NR1H3^{low}$ subgroups (Supplementary Figure S4A) also differed in terms of Mo infiltration, as inferred by CIBERSORTx. In fact, a significant predominance of M2 Mo was determined in the $NR1H3^{low}$ subgroup, whereas the M0/M1 Mo fraction prevailed in $NR1H3^{high}$ cases (Supplementary Figure S4B).

The digital measurement of *NR1H3* transcript in two independent DLBCL cohorts confirmed the prognostic performance of the gene according to a cut-off built on the discovery set. Moreover, the frequency of $NR1H3^{low}$ patients was consistent among both sets (12% and 16%, respectively) as well as their worse outcome compared with $NR1H3^{high}$ cases (Figure 2B–C). The multivariate models validated the independence of LXRα-based prognostication from COO and IPI risk (Figure 2B–C). Interestingly, while the transcriptional level of *NR1H3* differed significantly between on-trial cases (p-value $<10^{-3}$, Supplementary Figure S5A), the content of $CD68^{+}$ cells appeared quite comparable (p-value = 0.4176, Fisher's exact test) between $NR1H3^{high}$ and $NR1H3^{low}$ subgroups, supporting the idea that *NR1H3* reflects a transcriptional/functional rather than phenotypical heterogeneity of Mo within TME (Supplementary Figure S5 B-C). An additional validation attempt was carried out using a recent GEP dataset on a different platform (GSE117556, microarray technology), which highlight a dismal prognosis for $NR1H3^{low}$ patients, independently of IPI and COO risk groups (Supplementary Figure S6A).

Taken together, these findings strengthened the hypothesis that *NR1H3* levels characterize DLBCL with different outcomes reflecting diverse Mo subpopulations in their TME.

3.3 | *NR1H3* identifies DLBCL-infiltrating Mo with peculiar transcriptomic landscapes

To explore the molecular profiles associated with *NR1H3* in Mo in DLBCL, we sought to identify similarities and differences between virtually-purified Mo fractions of the $NR1H3^{high}$ and $NR1H3^{low}$ subgroups (Figure 3A). Considering as DEG those displaying a log fold change (FC) > 1 and an adjusted p-value <0.05, we obtained a total of 1040 up- and 169 down-regulated genes (Supplementary Table S2). To identify putative target genes of *NR1H3*, we intersected the obtained DEG (both up- and down-regulated) with 1079 LXRα targets from publicly available ChIP-seq data,[29] leading to the identification of 216 downstream targets. Gene Ontology analysis revealed genes enriched not only in the cholesterol and lipid metabolism, but also in inflammatory processes such as neutrophil activation, phagocytosis, cytokine production, and stimulation of innate immunity via toll-like receptors (Figure 3A–C). Gene set enrichment analysis also indicated that $NR1H3^{high}$ patients were significantly enriched of gene sets related to M1 phenotype (normalized enrichment score, NES = 1.8, p-value$<10^{-3}$), cytokines and inflammatory response (BIOCARTA_INFLAM_PATHWAY: NES = 1.8, p-value$<10^{3}$) including IL-6 and tumor necrosis factor, and immune functions such as antigen presentation (NES = 1.7, p-value = 0.002) (Figure 3D). A consistent enrichment of LXRα target genes (*ABCA1*, *ABCG1*, and *SREBF1*) was also noticeable, reflecting the transcriptional activity of the nuclear receptor (NES = 1.7, p-value$<10^{-3}$; Figure 3D).

Overall, these findings emphasized that LXRα-related signaling pathways and functions are associated with M1 polarization and potentially increased immune reactivity of Mo in DLBCL.

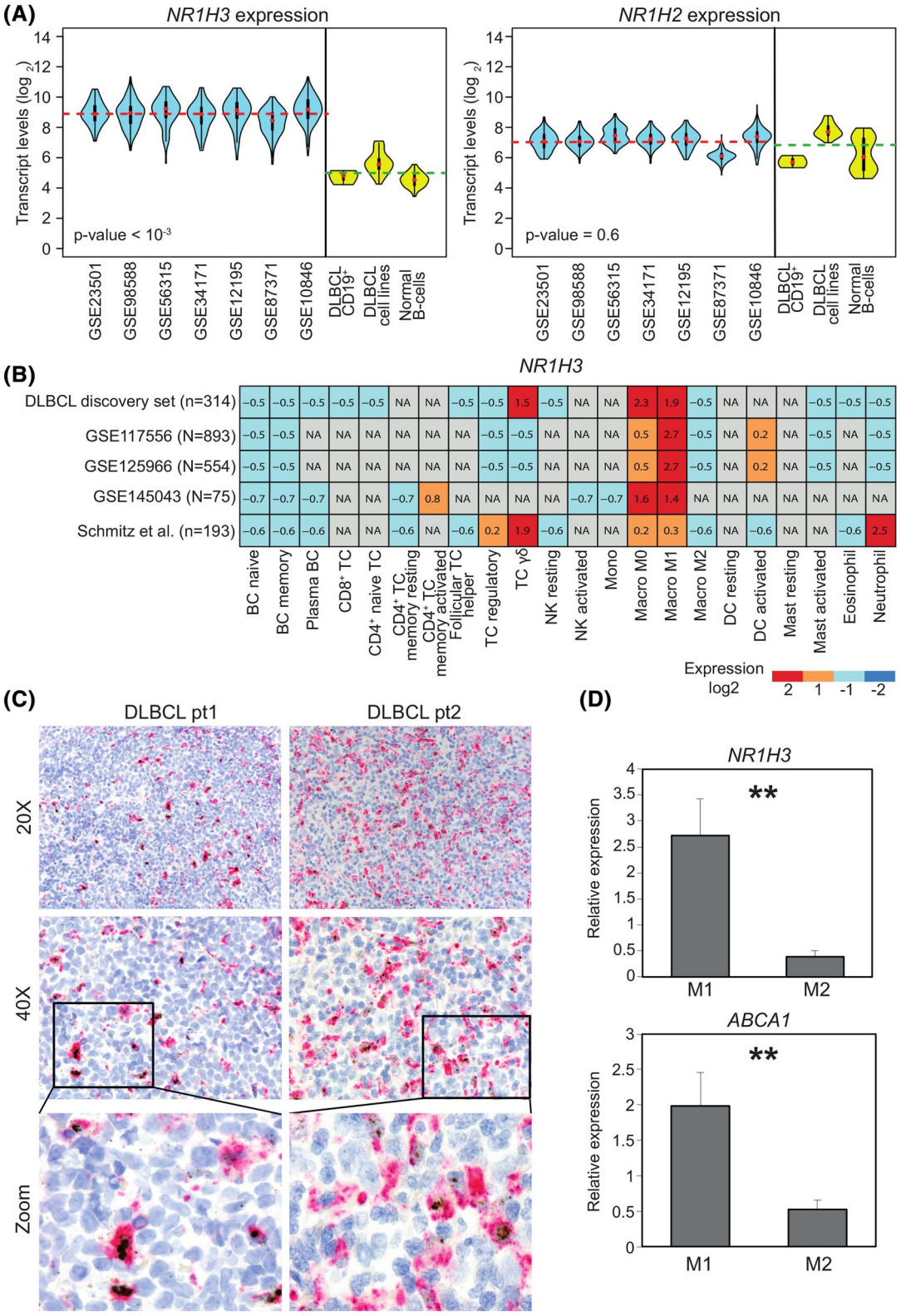

FIGURE 1 *NR1H3* is expressed by macrophages in diffuse large B-cell lymphomas (DLBCL). A, Violin-plots representing transcript abundance of *NR1H3* (left panel) and *NR1H2* (right panel) in publicly-available datasets from bulk tumor samples (light blue) or purified primary samples, DLBCL cell lines and normal B-cells (yellow). The gene expression omnibus accession numbers of DLBCL datasets are depicted in the *x*-axis. Dotted lines indicate *NR1H3* averaged expression respectively from bulk DLBCL samples (red) as well as purified DLBCL cell lines and normal B-cells (green), including germinal center centroblasts, naïve and memory B-cells (GSE12195 and GSE56314 datasets). *p*-value as derived from Mann–Whitney *U* test comparing bulk samples with purified cells is shown. B, Heatmap depicting *NR1H3* expression from *in silico* purification (CIBERSORTx) of different cell types five DLBCL datasets. Signal intensities ranking from highest (red) to

4 | DISCUSSION

Mo are essential elements of DLBCL microenvironment, but mechanisms underlying their prognostic significance remain unclear. Beyond correlating survival with the extent of Mo tumor infiltration, diverse methodologies - from IHC[30] to single-cell analyses of TME[31,32]- unveiled a remarkable heterogeneity of DLBCL-infiltrating Mo, at functional rather than phenotypic level.[23,31,32] However, no reproducible biomarker has been so far validated with a predictive value toward standard immunochemotherapy.

In this study, we expanded the notion of co-existing functional subsets of Mo within TME of DLBCL, revealing striking association of the LXRα transcript (encoded by *NR1H3* gene) expression with the M1 phenotype of Mo with putative anti-tumor effect. Accumulating data highlighted the relevance of LXRs in anti-cancer immune surveillance and described mechanisms of LXR axis activity in diverse immune cytotypes.[32,33] Particularly, the function of LXRα remains controversial as it can regulate a broad range of activities in specific subsets of accessory cells, such as Mo, in the context of various human cancers.[34] To dissect such biology in DLBCL, we exploited a high-resolution deconvolution of GEP from large patient cohorts and applied a discovery- validation approach using additional on trial and real-life case sets.

Compared with the reported literature, the identification of *NR1H3* as a reproducible, prognostic biomarker of functional Mo features overcomes existing phenotype-based methods to capture Mo heterogeneity. For instance, the prognostic use of CD68 immunostaining to estimate the histiocytic infiltration in DLBCL biopsies has produced inconsistent results[35–38] also due to the phenotypic nature of the marker, not being able to distinguish functionally-divergent Mo subsets. Conversely, when categorized according to *NR1H3* expression, DLBCL subgroups exhibit different enrichment of polarized Mo, with M1-like cells prevailing in *NR1H3*^{high} cohort, this being reflected by a more favorable outcome. We brought additional proof to this concept by measuring CD68^{+} cells in our on-trial validation set, where no significant difference emerged between prognostic subgroups despite divergent expression of LXR transcript. Such finding also stresses how the selection of functional immune biomarkers became essential to identify patient-specific TME for therapeutic purposes.

Deeper transcriptome-based approaches have revealed "stromal",[19] "mesenchymal", "inflammatory" and "lymphoma-associated macrophage" signatures with arguable significance in terms of prognostication, underlying biological mechanisms and clinical applicability.[39] In this context, the reported "lymphoma-associated macrophage interaction signature" (LAMIS)[9] was built in a supervised fashion on M2-related genes. The signature characterizes poor-outcome patients, but adds no further insights to previous evidence that greater CD163^{+} cell infiltration confers unfavorable prognosis.[38] A recent computational tool applied to thousands of DLBCL, named ECOTYPER, drew a high-resolution map of functional immune cell states and remarked heterogeneity in Mo population associating M1-like monocytes/Mo with longer survival, independently of current genomic prognosticators.[40] Such evidence is in line with ours and prompts to speculate whether the prevalence of pro-inflammatory Mo could boost the cytotoxicity of anti-CD20 therapy. Our results add up to this picture, providing reproducible evidence that a metabolic regulator, as LXRα, characterizes the M1-like subset of DLBCL-infiltrating Mo. Conversely, in low *NR1H3*-expressing patients likely prevails a different Mo-related biology which correlates with inferior outcome toward standard immunochemotherapy. We therefore envisage *NR1H3* as a potential biomarker for future strategies of immunomodulation. Beyond identifying patients at higher risk, in fact, the digital measurement of the transcript, according to the validated cut-off, may be of translational help in establishing preclinical patient-derived screening platforms for new immunotherapies.

Novel strategies are emerging aimed at reprogramming the innate immunity in many solid tumor models.[41] In fact, the LXRs activity can be modulated by synthetic agonists, including the recent developed RGX-104. This compound was already shown to exert remarkable anti-cancer effect in preclinical solid tumors[17,18] and it is being assessed for efficacy and safety in early clinical trials including aggressive lymphomas (ClinicalTrials.Gov, NCT02922764). Beside regulation of cholesterol homeostasis in Mo, LXR modulation was shown to affect secretion of cytokines impacting immune functions of T-regs,[42] natural killer cells,[43] myeloid-derived suppressor cells[18] and neutrophils[44] in both inflammatory diseases and cancer.[45] We also noticed a remarkable impact of *NR1H3* expression and its downstream targets on neutrophil-related processes as degranulation, activation and inflammatory response, suggesting intriguing interplay between Mo and other inflammatory bystander cells with potential effects on tumor behavior. Such hypothesis and the notion that both physiological activity of the receptor and its pharmacological modulation are tissue- and disease-specific,[46] prompt deeper mechanistic

lowest (blue) are indicated as row-scaled expression values. C, Representative histological sections of two DLBCL cases showing different levels of *NR1H3* transcript detected by RNA *in situ* hybridization (brown dots) and CD68 protein (magenta) by IHC using PG-M1 antibody (20X and 40X magnification depicted on left and right panel, respectively). The panels at the bottom are magnifications showing representative double-positive CD68^{+}/*NR1H3*$^{+}$ and single-positive CD68^{+}/*NR1H3*$^{-}$ cells. D, Bar plot representing *NR1H3* and *ABCA1* expression levels determined by quantitative real time polymerase chain reaction of *in vitro* generated Mo. Relative quantification of gene expression was analyzed by the $2^{-\Delta\Delta Ct}$ method using *18S* as the endogenous control. *p*-value was derived from two-tailed *t* test. Data are represented as the mean of four independent experiments ± SD (standard deviation). NA, not available

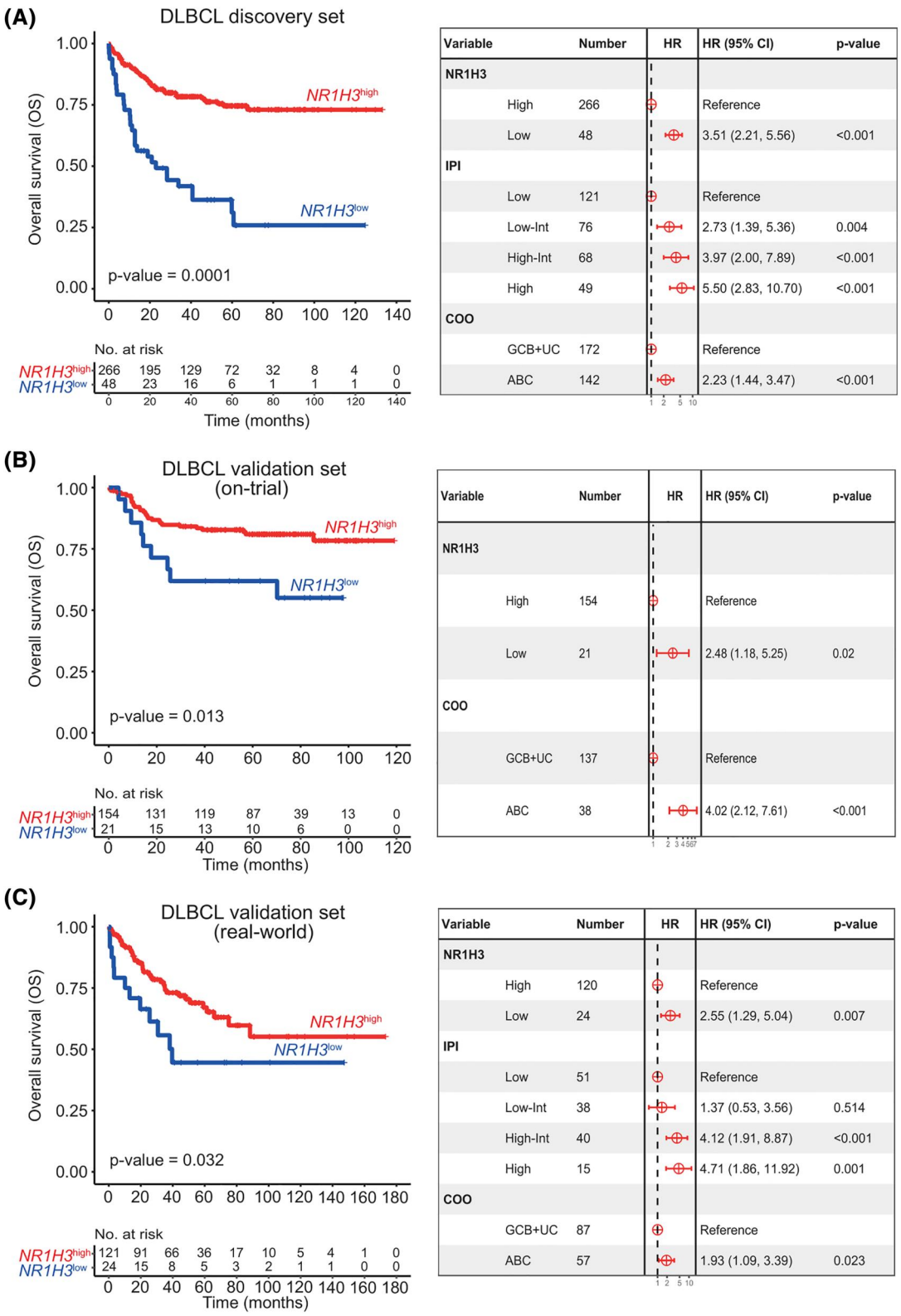

FIGURE 2 *NR1H3* prognostic significance in diffuse large B-cell lymphomas (DLBCL). A, Kaplan Meier (KM) plot (left panel) for overall survival (OS) according to *NR1H3*^{high} (red) and *NR1H3*^{low} (blue) groups derived from maximally selected rank statistic in the discovery set of 314 DLBCL. Forest plots (right panel) visualize HR and *p*-value obtained from multivariate analysis of *NR1H3* groups, cell of origin, COO and IPI of the discovery set. B, KM (left panel) plot of OS comparing high- versus low-*NR1H3* patients (NanoString Technology) in an on-trial validation cohort ($n = 175$). The right panel shows a Forest plot of multivariate analysis of OS combining *NR1H3* expression and COO. C, KM curves and Forest Plot for OS of the real-world validation cohort. KM plot displays different OS according to *NR1H3* expression subgroups, whereas Forest plot indicates multivariate analysis of *NR1H3* stratification, COO and IPI. Abbreviations: HR, hazard ratio; COO, cell of origin; IPI, international prognostic index

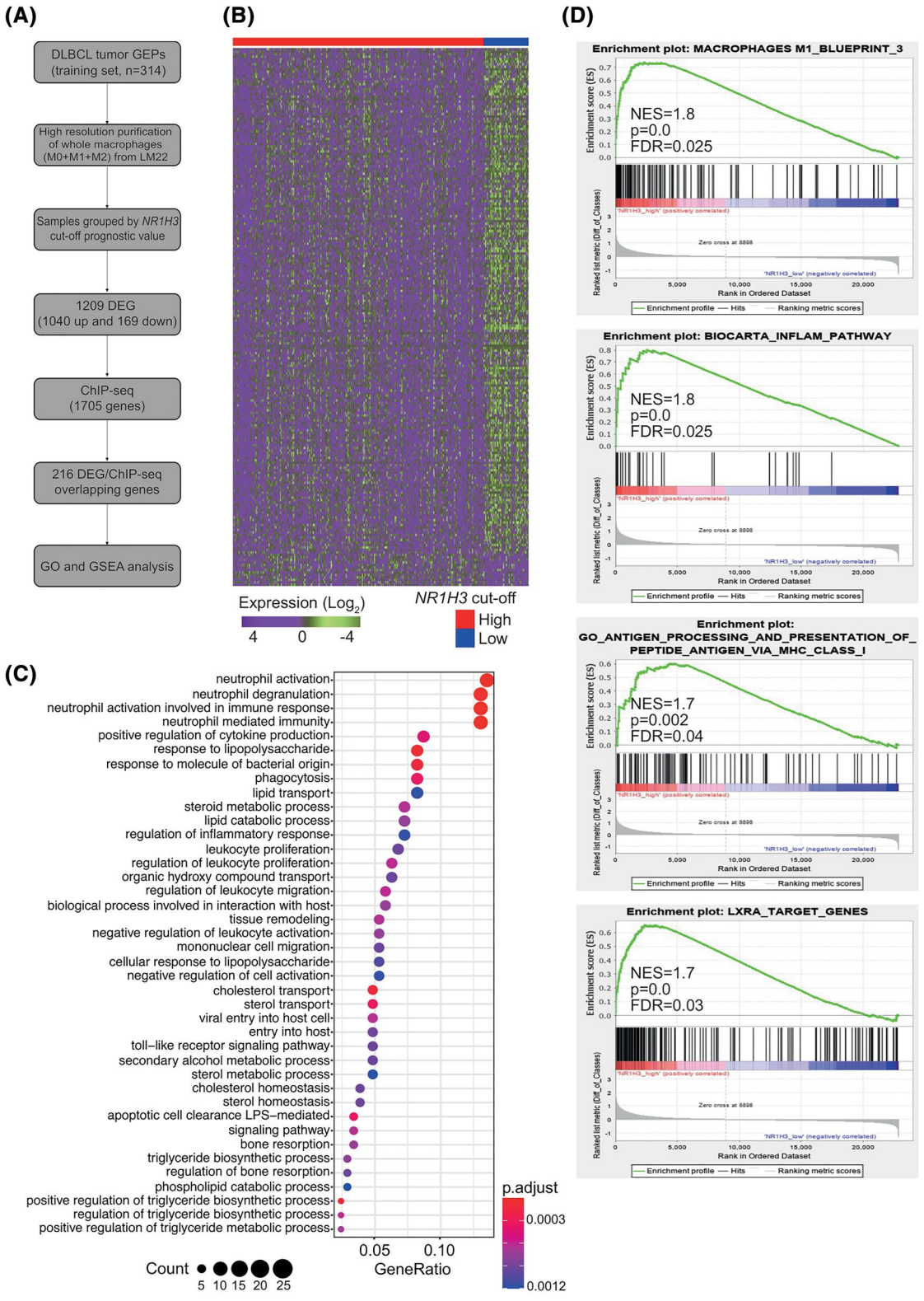

FIGURE 3 *NR1H3* defines functionally-restricted macrophages (Mo) subgroup in diffuse large B-cell lymphomas (DLBCL). A, Left panel schematizes the methodologic worflow applied to explore Mo biology in relation to *NR1H3*. Differentially expressed genes (DEG) were identified comparing samples grouped by *NR1H3* prognostic cut-off and overlapped with LXRα-target genes previously identified by ChIP-seq. B, Heatmap indicating 216 overlapping genes obtained from the discovery set by integrating microarray and ChIP-seq. Expression data were log_2-transformed and row-scaled. C, Dot-plot showing the top-30 significantly enriched biological processes derived by Gene Ontology (GO) analysis of 216 DEG-ChIP-seq overlapping genes in the discovery set. *p*-values adjusted using Benjamini-Hochberg procedure and gene counts are shown in the legend at the bottom. D, gene set enrichment analysis panels showing the enrichment of gene sets related to M1-macrophage subpopulation, inflammation and LXRα target genes in *NR1H3*^{high} cases from the discovery set. Abbreviations: DEG, differentially expressed genes; NES, normalized enrichment score; FDR, false discovery rate

investigation in more sophisticated pre-clinical models also resembling new genetic DLBCL subgroups.[5,6]

Overall, our study adds new understandings on the Mo heterogeneity in DLBCL, linking their metabolic diversity to functional divergence that could be captured by *NR1H3* as a reliable biomarker. The digital measurement of the receptor in diagnostic biopsy may also help in identifying *NR1H3*^{low} poor-outcome patients deserving alternative treatments. In conclusion, we provided the first comprehensive and disease-specific dissection of the role of LXRs in, promoting preclinical studies on the use of macrophage-targeted therapeutic strategies in DLBCL.

AUTHOR CONTRIBUTIONS

Maria Carmela Vegliante, Antonio Moschetta, Alessandro Gulino, Sabino Ciavarella and Stefano A. Pileri conceived and planned the project; Federica Melle, Giovanna Motta, Maria Rosaria Sapienza, Giuseppina Opinto, Anna Enjuanes, Antonella Bucci and Antonio Negri performed RNA extraction, digital expression analysis and in vitro experiments; AG, GM and produced in situ data, Maria Carmela Vegliante, Saveria Mazzara, Gian Maria Zaccaria, Simona De-Summa, Flavia Esposito, Giacomo Volpe and Grazia Gargano performed statistical analyses; Valentina Tabanelli, Stefano Fiori, Carla Minoia, Felice Clemente, Anna Scattone, Alfredo F. Zito, Stefania Tommasi, Claudio Agostinelli, Umberto Vitolo, Annalisa Chiappella, Anna Maria Barbui, Enrico Derenzini, Pier Luigi Zinzani, Beatrice Casadei, Alfredo Rivas-Delgado, Armando López-Guillermo, Elias Campo, Attilio Guarini and Stefano A. Pileri carried out samples collection, clinical annotation and pathology review; Maria Carmela Vegliante, Giacomo Volpe, Sabino Ciavarella and Stefano A. Pileri prepared the figures and wrote the manuscript; all authors critically reviewed the manuscript and approved the final draft for submission.

ACKNOWLEDGMENTS

This work was supported by grants from Associazione Italiana per la Ricerca sul Cancro (AIRC) (Fellowship 26928-2021 to GM, IG 23239 to AM and 5x1000 *n*. 21198 to SAP) and Italian Ministry of Health (Ricerca Corrente RRC-2019-2366660 to SC).

Open access funding provided by BIBLIOSAN.

CONFLICT OF INTEREST

ED, Research funding from TG-Therapeutics, ADC-Therapeutics, Takeda and Advisory board for Gilead, Astra Zeneca, Takeda, BeiGene, Abbvie. The other authors declare they have no conflicts of interest.

DATA AVAILABILITY STATEMENT

The data that support the findings of this study are available from the corresponding author upon reasonable request.

ORCID

Maria Rosaria Sapienza https://orcid.org/0000-0002-1078-2128
Stefania Tommasi https://orcid.org/0000-0002-2157-2978
Sabino Ciavarella https://orcid.org/0000-0003-4414-3903

PEER REVIEW

The peer review history for this article is available at https://publons.com/publon/10.1002/hon.3050.

REFERENCES

1. Swerdlow SH, World Health Organization, International Agency for Research on Cancer. WHO classification of tumours of haematopoietic and lymphoid tissues [Internet]. [cited 2018 Feb 15]. 585 p. http://publications.iarc.fr/Book-And-Report-Series/Who-Iarc-Classification-Of-Tumours/Who-Classification-Of-Tumours-Of-Haematopoietic-And-Lymphoid-Tissues-2017
2. Monti S, Chapuy B, Takeyama K, et al. Integrative analysis reveals an outcome-associated and targetable pattern of p53 and cell cycle deregulation in diffuse large B cell lymphoma. *Cancer Cell* Vol 22; 2012:.3359-372. [Internet][cited 2018 Jan 25]http://www.ncbi.nlm.nih.gov/pubmed/22975378
3. Morin RD, Mungall K, Pleasance E, et al. Mutational and structural analysis of diffuse large B-cell lymphoma using whole-genome sequencing. *Blood* Vol 122; 2013.7:1256-1265. [Internet][cited 2018 May 6]http://www.ncbi.nlm.nih.gov/pubmed/23699601
4. Reddy A, Zhang J, Davis NS, et al. Genetic and functional drivers of diffuse large B cell lymphoma. *Cell*. 2017;171(2):481-494. e15. https://doi.org/10.1016/j.cell.2017.09.027
5. Schmitz R, Wright GW, Huang DW, et al. Genetics and pathogenesis of diffuse large B-cell lymphoma. *N Engl J Med*. 2018;378(15):1396-1407. [Internet][cited 2018 Jun 24]http://www.nejm.org/doi/10.1056/NEJMoa1801445
6. Chapuy B, Stewart C, Dunford AJ, et al. Molecular subtypes of diffuse large B cell lymphoma are associated with distinct pathogenic mechanisms and outcomes. *Nat Med*. 2018;24(5):679-690. [Internet][cited 2018 Jun 24]Available from:. https://doi.org/10.1038/s41591-018-0016-8. http://www.ncbi.nlm.nih.gov/pubmed/29713087
7. Ciavarella S, Vegliante MC, Fabbri M, et al. Corrigendum: dissection of DLBCL microenvironment provides a gene expression-based predictor of survival applicable to formalin-fixed paraffin-embedded tissue. *Ann Oncol*. 2018;29(12):2363-2370. https://doi.org/10.1093/annonc/mdy450
8. Kotlov N, Bagaev A, Revuelta MV, et al. Clinical and biological subtypes of B-cell lymphoma revealed by microenvironmental signatures. *Cancer Discov*; 2021. [Internet]4 [cited 2021 Mar 17];candisc.0839.2020. https://cancerdiscovery.aacrjournals.org/content/early/2021/02/02/2159-8290.CD-20-0839
9. Staiger AM, Altenbuchinger M, Ziepert M, et al. A novel lymphoma-associated macrophage interaction signature (LAMIS) provides robust risk prognostication in diffuse large B-cell lymphoma clinical trial cohorts of the DSHNHL. *Leukemia*. 2019. [Internet] [cited 2019 Dec 19]; http://www.ncbi.nlm.nih.gov/pubmed/31530861
10. O'Neill LAJ, Pearce EJ. Immunometabolism governs dendritic cell and macrophage function. *J Exp Med*. 2016;213(1):15-23. https://doi.org/10.1084/jem.20151570. [cited 2018 May 6]. http://www.ncbi.nlm.nih.gov/pubmed/26694970
11. Repa JJ, Mangelsdorf DJ. The role of orphan nuclear receptors in the regulation of cholesterol homeostasis. *Annu Rev Cell Dev Biol*. 2000;16(1):459-481. [Internet][cited 2018 May 6]Available from:. https://doi.org/10.1146/annurev.cellbio.16.1.459. http://www.ncbi.nlm.nih.gov/pubmed/11031244
12. Bensinger SJ, Tontonoz P. Integration of metabolism and inflammation by lipid-activated nuclear receptors. *Nature*. 2008;454(7203):470-477. https://doi.org/10.1038/nature07202. [Internet][cited 2018 May 6]Available from:. http://www.ncbi.nlm.nih.gov/pubmed/18650918

13. Fontaine C, Rigamonti E, Nohara A, et al. Liver X receptor activation potentiates the lipopolysaccharide response in human macrophages. *Circ Res* Vol 101; 2007.1:40-49. 24 [cited 2018 May 6]. http://www.ncbi.nlm.nih.gov/pubmed/17540978
14. Bovenga F, Sabbà C, Moschetta A. Uncoupling nuclear receptor LXR and cholesterol metabolism in cancer. *Cell Metab* Vol 21; 2015.4: 517-526. [Internet][cited 2019 Oct 29]https://www.sciencedirect.com/science/article/pii/S1550413115001059?via%3Dihub
15. Pencheva N, Buss CG, Posada J, Merghoub T, Tavazoie SF. Broad-spectrum therapeutic suppression of metastatic melanoma through nuclear hormone receptor activation. *Cell* Vol 156; 2014.5: 986-1001. Cell [Internet][cited 2019 Oct 29]https://www.sciencedirect.com/science/article/pii/S0092867414000907?via%3Dihub
16. Nelson ER, Wardell SE, Jasper JS, et al. 27-Hydroxycholesterol links hypercholesterolemia and breast cancer pathophysiology. *Science*. 2013;342(6162):1094-1098. [Internet]. 2013 Nov 29 [cited 2021 Aug 26]Available from:. https://doi.org/10.1126/science.1241908. https://science.sciencemag.org/content/342/6162/1094
17. Mita MM, Mita AC, Chmielowski B, et al. Pharmacodynamic and clinical activity of RGX-104, a first-in-class immunotherapy targeting the liver-X nuclear hormone receptor (LXR), in patients with refractory malignancies. *J Clin Oncol*. 2018;36(15_Suppl I):3095. https://doi.org/10.1200/jco.2018.36.15_suppl.3095
18. Tavazoie MF, Pollack I, Tanqueco R, et al. LXR/ApoE activation restricts innate immune suppression in cancer. *Cell*. 2018;172(4): 825-840. e18. https://doi.org/10.1016/j.cell.2017.12.026
19. Lenz G, Wright G, Dave SS, et al. Stromal gene signatures in large-B-cell lymphomas. *N Engl J Med*. Vol 359; 2008.22:2313-2323. [Internet][cited 2017 Dec 19]http://www.nejm.org/doi/abs/10.1056/NEJMoa0802885
20. Chiappella A, Martelli M, Angelucci E, et al. Rituximab-dose-dense chemotherapy with or without high-dose chemotherapy plus autologous stem-cell transplantation in high-risk diffuse large B-cell lymphoma (DLCL04): final results of a multicentre, open-label, randomised, controlled, phase 3 study. *Lancet Oncol*; 2017. 18(8):1076–1088. [Internet][cited 2018 Jan 8]. http://www.ncbi.nlm.nih.gov/pubmed/28668386
21. Cortelazzo S, Tarella C, Gianni AM, et al. Randomized trial comparing R-CHOP versus high-dose sequential chemotherapy in high-risk patients with diffuse large B-cell lymphomas. *J Clin Oncol*. 2016;34(33):4015–4022. [Internet][cited 2018 Jan 8];34(33):4015–22. http://www.ncbi.nlm.nih.gov/pubmed/28199143
22. Sha C, Barrans S, Cucco F, et al. Molecular high-grade B-cell lymphoma: defining a poor-risk group that requires different approaches to therapy. *J Clin Oncol*. 2019;37(3):202–212. [cited 2019 Oct 29]. http://www.ncbi.nlm.nih.gov/pubmed/30523719
23. Shaknovich R, Geng H, Johnson NA, et al. DNA methylation signatures define molecular subtypes of diffuse large B-cell lymphoma. *Blood*; 2010;116(20):e81-e89. [Internet][cited 2019 Feb 19]. http://www.ncbi.nlm.nih.gov/pubmed/20610814
24. Dybkær K, Bøgsted M, Falgreen S, et al. Diffuse large B-cell lymphoma classification system that associates normal B-cell subset phenotypes with prognosis. *J Clin Oncol*. 2015. [cited 2022 Jan 27];33(12):1379–88. https://pubmed.ncbi.nlm.nih.gov/25800755/
25. Dubois S, Viailly PJ, Bohers E, et al. Biological and clinical relevance of associated genomic alterations in MYD88 L265P and non-L265P-mutated diffuse large B-cell lymphoma: Analysis of 361 cases. *Clin Cancer Res*; 2017;23(9):2232–2244. [cited 2022 Jan 27];23(9):2232–44. https://pubmed.ncbi.nlm.nih.gov/27923841/
26. Kotlov N, Bagaev A, Revuelta MV, et al. Clinical and biological subtypes of b-cell lymphoma revealed by microenvironmental signatures. *Cancer Discov*; 2021;11(6):1468–1489. [Internet][cited 2021 Jun 8];http://cancerdiscovery.aacrjournals.org/
27. Ciavarella S, Vegliante MC, Fabbri M, et al. Dissection of DLBCL microenvironment provides a gene expression-based predictor of survival applicable to formalin-fixed paraffin-embedded tissue. *Ann Oncol*. 2018;29(12):2363-2370. https://doi.org/10.1093/annonc/mdy450
28. Tjiu J.-W, Chen J.-S, Shun C.-T, et al. Tumor-associated macrophage-induced invasion and angiogenesis of human basal cell carcinoma cells by cyclooxygenase-2 induction. *J Invest Dermatol*. 2009;129(4): 1016–1025. [Internet][cited 2018 May 14]. http://linkinghub.elsevier.com/retrieve/pii/S0022202X15342901
29. Feldmann R, Fischer C, Kodelja V, et al. Genome-wide analysis of LXRα activation reveals new transcriptional networks in human atherosclerotic foam cells. *Nucleic Acids Res*. 2013;41(6):3518–3531. [Internet][cited 2021 Aug 26]. https://pubmed.ncbi.nlm.nih.gov/23393188/
30. Croci GA, Au-Yeung RKH, Reinke S, et al. SPARC positive macrophages are the superior prognostic factor in the microenvironment of diffuse large B-cell lymphoma and independent of MYC rearrangement and double/triple hit status. *Ann Oncol*; 2021. [Internet][cited 2021 Aug 26];0(0). https://linkinghub.elsevier.com/retrieve/pii/S0923753421042757
31. Bruns H, Büttner M, Fabri M, et al. Vitamin D–dependent induction of cathelicidin in human macrophages results in cytotoxicity against high-grade B cell lymphoma. *Sci Transl Med*. 2015;7(282). [Internet][cited 2018 May 6];7(282):282ra47-282ra47. Available from:. https://doi.org/10.1126/scitranslmed.aaa3230. http://www.ncbi.nlm.nih.gov/pubmed/25855493
32. Bilotta MT, Petillo S, Santoni A, Cippitelli M. Liver X receptors: regulators of cholesterol metabolism, inflammation, autoimmunity, and cancer. *Front Immuno*. Vol 11:2020:2867.
33. Brendolan A, Russo V. Targeting cholesterol homeostasis in hematopoietic malignancies. *Blood*; 2021;139(2). [Internet][cited 2022 Jan 14];139(2). https://pubmed.ncbi.nlm.nih.gov/34610110/
34. Derangère V, Chevriaux A, Courtaut F, et al. Liver X receptor β activation induces pyroptosis of human and murine colon cancer cells. *Cell Death Differ*. 2014;21(12):1914-1924. [Internet][cited 2021 Dec 22];21(12):1914–24. Available from:. https://doi.org/10.1038/cdd.2014.117. https://pubmed.ncbi.nlm.nih.gov/25124554/
35. Riihijärvi S, Fiskvik I, Taskinen M, et al. Prognostic influence of macrophages in patients with diffuse large B-cell lymphoma: a correlative study from a Nordic phase II trial. *Haematologica*; 2015;100(2):238–245. Haematologica [Internet][cited 2018 Jan 8];100(2):238–45. http://www.ncbi.nlm.nih.gov/pubmed/25381134
36. Nam SJ, Go H, Paik JH, et al. An increase of M2 macrophages predicts poor prognosis in patients with diffuse large B-cell lymphoma treated with rituximab, cyclophosphamide, doxorubicin, vincristine and prednisone. *Leuk Lymphoma*. 2014;55(11):2466–2476. http://www.ncbi.nlm.nih.gov/pubmed/24397616
37. Wada N, Zaki MAA, Hori Y, et al. Tumour-associated macrophages in diffuse large B-cell lymphoma: a study of the osaka lymphoma study group. *Histopathology*; 2012;60(2):313–319. Histopathology [Internet][cited 2018 May 6];60(2):313–9. http://www.ncbi.nlm.nih.gov/pubmed/22211289
38. Marchesi F, Cirillo M, Bianchi A, et al. High density of CD68+/CD163+ tumour-associated macrophages (M2-TAM) at diagnosis is significantly correlated to unfavorable prognostic factors and to poor clinical outcomes in patients with diffuse large B-cell lymphoma. *Hematol Oncol*; 2015;33(2):110–112. [Internet][cited 2018 May 6];33(2):110–2. http://www.ncbi.nlm.nih.gov/pubmed/24711044
39. Kotlov N, Bagaev A, Revuelta MV, et al. Clinical and biological subtypes of b-cell lymphoma revealed by microenvironmental signatures. *Cancer Discov*; 2021;11(6):1468–1489. [Internet][cited 2021 Oct 19];11(6):1468–89. http://cancerdiscovery.aacrjournals.org/
40. Steen CB, Luca BA, Esfahani MS, et al. The landscape of tumor cell states and ecosystems in diffuse large B cell lymphoma. *Cancer Cell*;

2021:1422-1437. [Internet][cited 2021 Oct 19];39(10)e10. https://linkinghub.elsevier.com/retrieve/pii/S1535610821004517
41. Sun L, Kees T, Almeida AS, et al. Activating a collaborative innate-adaptive immune response to control metastasis. *Cancer Cell*; 2021:1361-1374. [Internet][cited 2021 Oct 19];39(10)e9. https://pubmed.ncbi.nlm.nih.gov/34478639/
42. Herold M, Breuer J, Hucke S, et al. Liver X receptor activation promotes differentiation of regulatory T cells. *PLoS One* Vol 12; 2017;e0184985. [Internet][cited 2021 Dec 22]https://dx.plos.org/10.1371/journal.pone.0184985
43. Bilotta MT, Abruzzese MP, Molfetta R, et al. Activation of liver X receptor up-regulates the expression of the NKG2D ligands MICA and MICB in multiple myeloma through different molecular mechanisms. *FASEB J*. 2019;33(8):9489-9504. [Internet][cited 2021 Dec 22];33(8):9489–504. https://onlinelibrary.wiley.com/doi/10.1096/fj.201900319R
44. Badea L, Herlea V, Dima SO, Dumitrascu T, Popescu I. Combined gene expression analysis of whole-tissue and microdissected pancreatic ductal adenocarcinoma identifies genes specifically overexpressed in tumor epithelia. *Hepatogastroenterology*. 55(88): 2016–2027. [Internet]. [cited 2018 Oct 10];55(88):2016–27. http://www.ncbi.nlm.nih.gov/pubmed/19260470
45. González De La Aleja1 A, De La Rosa JV, Alonso B, Puig-Kroger A, Vega MA, Corbi AL. LXR nuclear receptors prompt a pro-innammatory gene and functional proole in human macrophages; 2021. [cited 2022 Jan 25]; https://www.researchsquare.com
46. Raccosta L, Fontana R, Maggioni D, et al. The oxysterol-cxcr2 axis plays a key role in the recruitment of tumor-promoting neutrophils. *J Exp Med*. 2013. 10(9):1711–1728 [Internet][cited 2021 Dec 22]; 210(9):1711–28. Available from: http://pmc/articles/PMC3754872/

SUPPORTING INFORMATION

Additional supporting information can be found online in the Supporting Information section at the end of this article.

How to cite this article: Vegliante MC, Mazzara S, Zaccaria GM, et al. *NR1H3* (LXRα) is associated with pro-inflammatory macrophages, predicts survival and suggests potential therapeutic rationales in diffuse large b-cell lymphoma. *Hematol Oncol*. 2022;40(5):864-875. https://doi.org/10.1002/hon.3050